Evolution of seawater continentally-sourced Nd isotopic composition prior to and during the Great Oxidation Event

Francesco Narduzzi, Delphine Bosch, Pascal Philippot

Evolution of seawater continentally-sourced Nd isotopic composition prior to and during the Great Oxidation Event

Francesco Narduzzi [a,b,*], Delphine Bosch [a], Pascal Philippot [a,b]

[a] Géosciences Montpellier, Université de Montpellier, CNRS, 34095 Montpellier, France
[b] Instituto de Astronomia, Geofísica e Ciências Atmosféricas da Universidade de São Paulo – IAG-USP, Rua do Matão, 1226 – Cidade Universitária, Butantã, 05508-090 São Paulo – SP, Brazil

ARTICLE INFO

Keywords:
Hamersley Basin
Weathering of exposed continental landmasses
Nd isotopes
Subaerial Large Igneous Provinces
Great Oxidation Event
Paleoproterozoic Glaciations

ABSTRACT

An ongoing debate concerns what initiated the Great Oxidation Event (GOE) and associated glaciation between ~ 2.45 and 2.2 Ga. One possibility is the emergence of continental landmasses and the increase of subaerial igneous province weathering during the Late Archean. We test this hypothesis in the Hamersley Basin by reporting Nd-isotope data from a succession of iron formations (IFs), mudstone/siltstones and glacial diamictites from the Boolgeeda Iron Formation and overlying Turee Creek Group deposited during the GOE. In a $^{147}Sm/^{144}Nd$ - $\varepsilon Nd_{(t)}$ diagram, the data define a negative trend indicating the contribution of a high $\varepsilon Nd_{(t)} \sim +3$ hydrothermal component and a strongly negative $\varepsilon Nd_{(t)} \sim -9$ crustal component, which is compatible with the Nd-isotope composition of the upper continental crust but also of the underlying felsic volcanics of the Woongarra Rhyolite and crustally-contaminated mafic volcanics of the Fortescue Group. A less pronounced negative trend originating from the same hydrothermal source but correlated with non-contaminated ultramafic Fortescue volcanics ($\varepsilon Nd_{(t)} \sim -2$) is observed for the older Joffre, Dales Gorge and Marra Mamba IFs. As Nd-isotopes are not sensitive to redox conditions, the major shift of Nd-isotopic compositions at ~ 2.45 Ga cannot be linked to a change in the weathering regime, rather to a change in the nature of the continental surface exposed to weathering. One explanation is that the Sm-Nd sources for sediments deposited before and during the GOE were locally derived from the underlying subaerial LIPs, reflecting a change in the geodynamic context of deposition and/or hydrographic network and catchment areas. Another explanation could be a significant change in the nature of fluid–rock interactions due to the increase role of weathering processes associated with the emergence of continental landmasses. Additional Nd isotope data from different cratons worldwide are needed, however, to infer as to whether or not the marked shift in Nd isotope compositions recorded in the Turee Creek Group reflect a change in the global hydrological cycle. Our data support the role of large subaerial magmatic provinces as triggers of the rise of atmospheric oxygen and the onset of glaciations at the beginning of the Proterozoic.

1. Introduction

Between about 2.45 and 2.2 Ga, the Great Oxidation Event (GOE) and associated phase of global cooling that led to the first snowball Earth event represent one of the most significant changes in Earth's surface chemistry and redox state through time (Holland, 2002; Hoffman, 2013). In recent years, numerous studies have emphasized the influence of Earth's internal geodynamics on surface processes (Barley et al., 2005; Kump and Barley, 2007; Flament et al., 2008; Rey and Coltice, 2008; Cox et al., 2016; Bindeman et al., 2018). Among these, Kump and Barley (2007) explained the rise of atmospheric oxygen and associated decrease of surface temperature by a change in the eruptive dynamic of the Earth at ca. 2.5 Ga, which shifted the main volcanism style from marine to subaerial. This increase in the subaerial proportion of Large Igneous Provinces (LIPs) would have increased weathering and the flux of nutrients to the continents, buffered the concentration of atmospheric carbon dioxide and ultimately contributed to the global cooling of the planet and the build-up of atmospheric O_2 (Kump and Barley, 2007; Catling and Claire, 2005; Claire et al., 2006; Teitler et al., 2014; Bindeman et al., 2018). In addition, subaerial volcanic eruptions are known to produce more oxidized lavas and gases (Holland, 2002; Gaillard et al., 2011), which could also have contributed further to lower

* Corresponding author at: Instituto de Astronomia, Geofísica e Ciências Atmosféricas da Universidade de São Paulo – IAG-USP, Rua do Matão, 1226 – Cidade Universitária, Butantã, 05508-090 São Paulo – SP, Brazil.
E-mail address: narduzzi13@gmail.com (F. Narduzzi).

oxygen sinks. Because Late Archean – Early Proterozoic LIPs have chemical compositions that are distinct from average continental crust and show similar or slightly older age than the sediments deposited during the GOE, massive chemical and physical weathering of these LIPs should leave a specific imprint in the sedimentary record.

We present here Nd-isotope and trace element measurements of chemical (iron formations) and detrital (mudstones, siltstones and glacial diamictites) sediments from the 2.45 to 2.2 Ga old Turee Creek Group and the conformably underlying Boolgeeda Iron Formation of the Hamersley Group, Western Australia. The Boolgeeda IF is composed of mixed chemical and siliciclastic components (green mudstones and one glacial horizon; Philippot et al., 2018; Warchola et al., 2018) and therefore can be used to constrain the bulk composition of seawater but also the composition of the emergent continental landmasses during the first major glacial event at about 2.45 Ga. The Turee Creek Group sediments are siliciclastic sediments (mudstone/siltstones and glacial diamictites) spanning the GOE and at least two other glacial episodes and therefore can be used to track the evolution of the continental crustal source during the rise of atmospheric oxygen (Van Kranendonk and Mazumder, 2015; Caquineau et al., 2018, 2020). The data obtained are compared with previously published Nd-isotope data from IFs and associated siliciclastic sediments from the Hamersley Group (Joffre, Dales Gorge and Marra Mamba formations; Miller and O'Nions, 1985; Jacobsen and Pimentel-Klose, 1988; Alibert and McCulloch, 1993; Li et al., 2015) as well as mafic and felsic subaerial volcanic rocks from the Woongarra, Weeli Wolly and Fortescue LIPs (Macfarlane et al., 1994a, 1994b; Trendall, 1995; Mole et al., 2018 and GSWA WAGeochem database) of the Hamersley and Fortescue groups. Together the data reveal a dominant contribution of subaerial LIPs weathering to both detrital and solute fluxes during deposition of the different iron formations. They also point to a major change in the nature of the materials delivered to the ocean at the onset of the GOE.

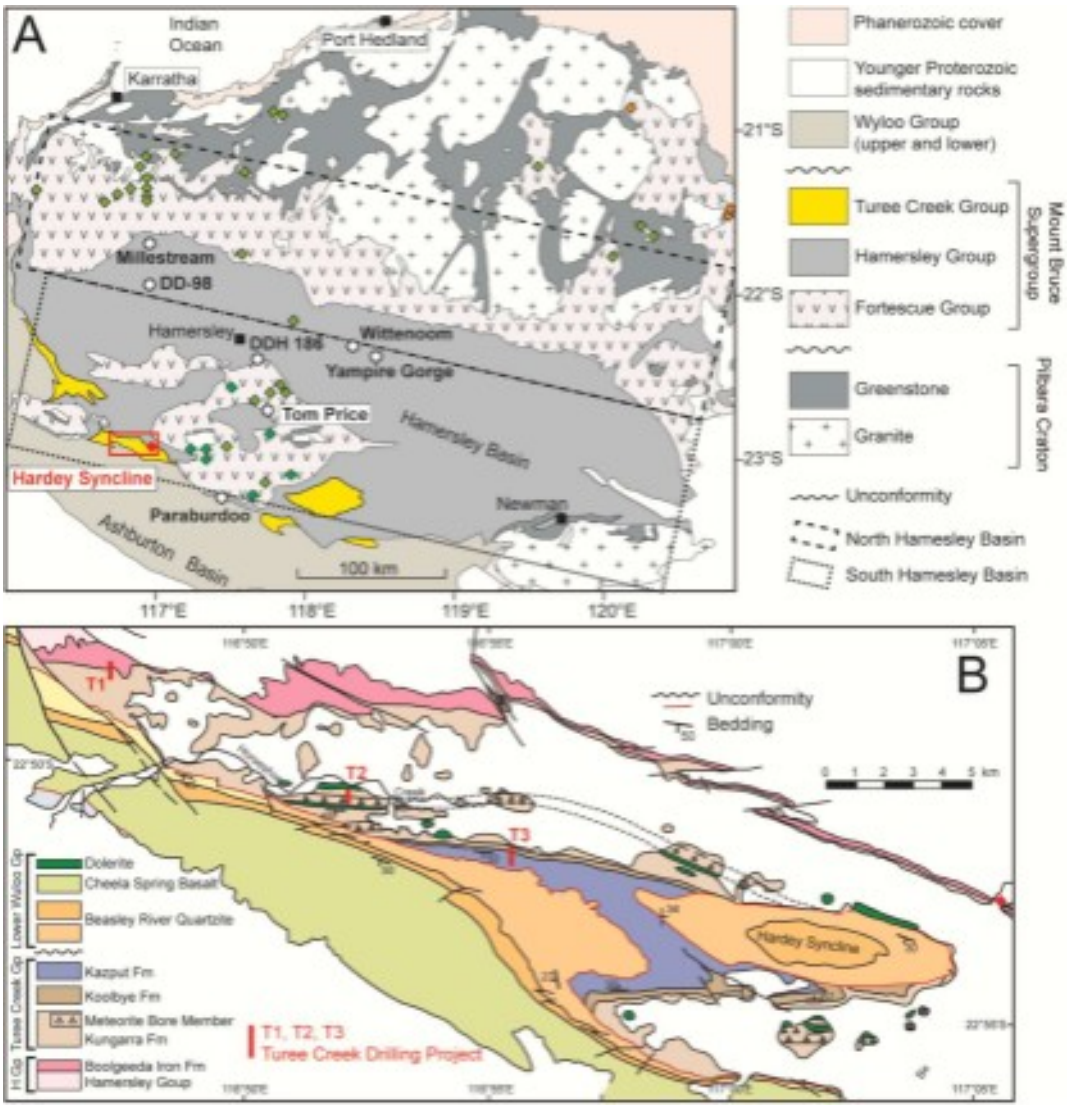

Fig. 1. (A) Geological map of the Pilbara Craton and associated Hamersley Basin and Turee Creek Group (modified from Philippot et al., 2018). The red rectangle points to the Hardey Syncline (Fig. 1B) where the Turee Creek Drilling Project was conducted. Sampling location for Marra Mamba, Dales Gorge and Joffre IFs are shown as white circles (see Alibert and McCulloch, 1993; Haugaard et al., 2016; Li et al., 2015; Pecoits et al., 2009). Location of the Fortescue volcanic rocks for which Nd isotopes are available (Macfarlane et al., 1994b; Mole et al., 2018 and references therein) are shown as: crustally-contaminated basalts (light green diamonds), Pyradie komatiites (dark green diamonds) and felsic volcanics (orange diamonds). Note that each symbol can represent more than one sample. A unique sample of the 2.45 Ga Woongarra Rhyolite (GSWA WAGeochem database) is shown as red diamond. (B) Geological map of the Hardey Syncline showing the location of T1, T2 and T3 drill holes. Note the red diamond in the upper right side indicating the location of the Woogarra Rhyolite analyzed for its Nd-isotope composition. (For interpretation of the references to colour in this figure legend, the reader is referred to the web version of this article.)

2. Geological background

The Turee Creek Group (TCG) is a ~ 4 km-thick continuous sedimentary rock succession located stratigraphically at the top of the Mount Bruce Supergroup (Figs. 1 and 2). The TCG is conformably overlying the Hamersley and Fortescue groups and unconformably underlying the Beasley River Quartzite, which forms the base of the Wyloo Group (Fig. 1A, 1B and 2A; Trendall, 1979; Arndt et al., 1991; Trendall et al., 2004). From bottom to top, the TCG consists of siliciclastic sedimentary rocks, minor stromatolitic carbonates and two glaciogenic strata (Meteorite Bore Member, MBM1 and MBM2) of the Kungarra Formation, quartz-rich sandstones of the Koolbye Formation, and shales and stromatolitic marine carbonates of the Kazput Formation (Fig. 2B and C; Martin, 1999; Trendall et al., 2004; Van Kranendonk et al., 2015). The TCG conformably overlies the Boolgeeda IF of the underlying Hamersley Group. This sedimentary succession has been described as a broad shallowing upward profile from deep-water iron formation of the Boolgeeda IF, through fine-grained siliciclastic deposits of the Kungarra Formation, to fluvial and shallow marine strata of the Koolbye and Kazput formations (Martin, 1999; Mazumder et al., 2015; Van Kranendonk et al., 2015). The Boolgeeda Iron Formation overlies the Woongarra Rhyolite and Weeli Wooli Formation, which have been interpreted as a subaerial bimodal mafic and felsic volcanic sequence emplaced at 2450 Ma (Barley et al., 1997). This intense volcanic event would have produced large volumes of lavas covering the continental surface at the time of the glacial event recorded in the Boolgeeda Iron Formation, and possibly during the subsequent deposition of the overlying TCG. Metamorphism did not exceed sub-greenschist facies conditions (Rasmussen et al., 2005). Time constraints on the deposition of the Boolgeeda IF and TCG include a U-Pb zircon age of 2455 ± 3 Ma for the underlying Woongarra Rhyolite (Trendall et al., 2004), a maximum U-Pb detrital zircon age of 2460 ± 9 Ma for the Boolgeeda diamictite (Caquineau et al., 2018), a Re-Os age of 2313 ± 6 Ma obtained on diagenetic pyrite from the Meteorite Bore Member diamictite of the TCG (Philippot et al., 2018) in agreement with a maximum U-Pb age on detrital zircon of 2340 ± 22 Ma (Caquineau et al., 2018) for this glacial formation (Fig. 2A). The age of the overlying Beasley River Quartzite is loosely bracketed between ~ 2210 Ma and 2031 ± 6 Ma (Martin et al., 1998; Müller et al., 2005).

The more generally accepted scenario for the formation of the Turee Creek Basin considers a long-lived basin that formed between ~ 2.45 and 2.2 Ga (e.g., Martin et al., 2000; Van Kranendonk et al., 2015; Caquineau et al., 2018). Combining U-Pb dating and Hf isotopes of detrital zircons, Caquineau et al. (2020) recently showed that the Boolgeeda IF and TCG sediments mainly derived from the erosion of the underlying Hamersley and Fortescue groups, which are formed by a variety of sedimentary successions interleaved with thick subaerial volcanic sequences.

3. Methods and results

3.1. Analyzed samples

The samples used here are the same as those used in previous studies (Caquineau et al., 2018; Philippot et al., 2018; Warchola et al., 2018; Cheng et al., 2019; Killingsworth et al., 2019). These include samples collected in three drill cores obtained in the course of the Turee Creek Drilling Project (TCDP) that intercept representative stratigraphic sections at the base (Boolgeeda–Kungarra transition, TCDP 1), middle (MBM1 diamictite and underlying Kungarra shales and carbonates, TCDP 2), and top (Kazput–Koolbye transition, TCDP 3) of the Hamersley and Turee Creek groups (Figs. 1 and 2; see Philippot et al., 2018 for details). Nd-isotope composition was measured on 21 samples from the Boolgeeda IF and 11 samples from the TCG (Fig. 2C, Supplementary Table S1). Precise Sm and Nd contents for the TCG samples were determined in this study while those for the Boolgeeda IF are from Warchola et al. (2018). Sm and Nd content analyses are those described in Warchola et al. (2018).

3.2. Analytical techniques

Depending on the elemental Nd content of the sample, powdered samples were weighed in Savillex™ Teflon beakers in order to obtain between 100 and 300 ng of Nd. Then, 0.5 ml of 2.5 M HCl was added and the samples were placed on a hotplate at 90 °C for 1 h for a gentle oxidation step. Samples were then dissolved using a mixture of 28 M HF, 13 M HNO_3 and $HClO_4$ in 1:1:0.1 proportions and placed on the hotplate at 140 °C for at least 72 h. After evaporation to dryness at 90 °C, 2 ml of HNO_3 was added to the residue and the samples replaced at 95 °C for 48 h before the samples were dried down. In order to separate Nd, alkalis, REEs and HFSEs were successively and separately pre-concentrated using Teflon column filled with cation-exchange resin (AG50 W-X8 200–400 mesh). Nd was then purified from other REEs using home-made pure Quartz columns filled with HDEHP-coated Teflon powder and using tri-distilled 0.3 N HCl as eluants. The total Nd procedural blanks were measured during each chemical separation batch and were lower than 8 pg.

Nd-isotope ratios were measured at Geoscience Montpellier using a Thermo Scientific Neptune Plus MC-ICP-MS (AETE-ISO platform of the OSU OREME). Analyses were done during three distinct sessions, all within April 2019. $^{143}Nd/^{144}Nd$ isotopic compositions were corrected from internal mass bias using a value of 0.7219 for the $^{146}Nd/^{144}Nd$ ratio. In order to evaluate the reproducibility and accuracy of isotopic measurements during the analyses, both AMES-Rennes ($^{143}Nd/^{144}Nd$ = 0.511961 ± 0.000013 (2σ); Chauvel and Blichert-Toft, 2001) and JMC-321 Nd standard ($^{143}Nd/^{144}Nd$ = 0.511105 ± 0.000013 (2σ)) were measured in bracketing mode between 2 unknowns. Compilation of the analytical results obtained for the standards during the course of this study is reported in Supplementary Table S2. Initial $^{143}Nd/^{144}Nd$ isotopic ratios for Boolgeeda IF and TCG samples were corrected at 2.45 Ga (Trendall et al., 2004; Caquineau et al., 2018) and at 2.31 Ga (Philippot et al., 2018), respectively.

3.3. Results

Figs. 2 and 3 show that the Boolgeeda samples yield a wide range of $^{147}Sm/^{144}Nd$ values between 0.093 and 0.145, which encompasses the significantly smaller range of values obtained for the TCG samples between 0.107 and 0.118. $\varepsilon Nd_{(t)}$ values of the Boolgeeda samples show a wide range between + 4.2 and −8.9, whereas the TCG samples show a much limited negative range from −4.4 to −8.4 (Fig. 2C). Boolgeeda Al-poor IFs show $\varepsilon Nd_{(t)}$ values between −2.4 and −8.3 and $^{147}Sm/^{144}Nd$ ratios of 0.101 and 0.129. The Al-rich IFs show a trend from near-chondritic ($\varepsilon Nd_{(t)}$ = +0.4) to crustal ($\varepsilon Nd_{(t)}$ = -8.1) values coupled with an increase of $^{147}Sm/^{144}Nd$ ratios from 0.105 to 0.145. Green mudstones show a rather constant $^{147}Sm/^{144}Nd$ ratio from 0.110 to 0.119, but a $\varepsilon Nd_{(t)}$ variability from + 0.2 to −8.9 compatible with the other Boolgeeda samples. One of the two Boolgeda cherts yields the highest $\varepsilon Nd_{(t)}$ value of our dataset that overlaps the HT hydrothermal field (Fig. 3A). The Boolgeeda and MBM1 glacial diamictites show similar $^{147}Sm/^{144}Nd$ ratios but substantially different $\varepsilon Nd_{(t)}$ values from −3.0 to −1.7 and −6.9 to −5.8, respectively (Fig. 2C). In all three drill cores, the TCG mudstone/siltstones show relatively homogeneous $^{147}Sm/^{144}Nd$ ratios with $\varepsilon Nd_{(t)}$ values from − 4.4 to − 8.4.

4. Discussion

4.1. Boolgeeda and Turee Creek sediments

In a $\varepsilon Nd_{(t)}$ vs $^{147}Sm/^{144}Nd$ diagram, the TCG and Boolgeeda samples define a steep negative trend characterized by a restricted range of $^{147}Sm/^{144}Nd$ ratios but a variable range in $\varepsilon Nd_{(t)}$ values between −8.4

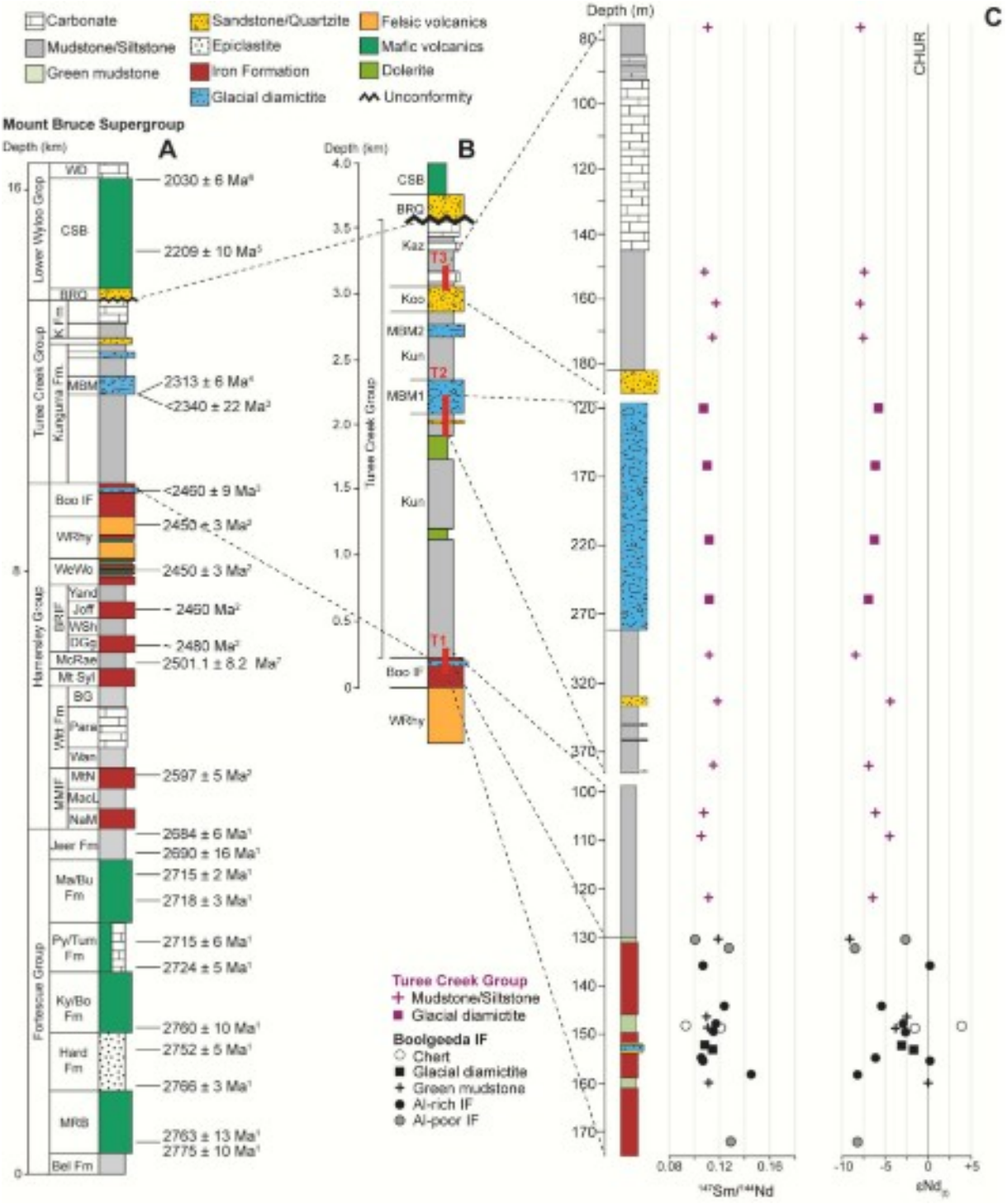

Fig. 2. Lithostratigraphy of the Mount Bruce Supergroup (A) and Turee Creek Group and Boolgeeda IF and associated Turee Creek drill holes T1, T2 and T3 (B) (modified after Trendall et al., 2004; Philippot et al., 2018). In (A) ages constraints are from: (1) Mole et al. (2018), (2) Trendall et al. (2004), (3) Caquineau et al. (2018), (4) Philippot et al. (2018), (5) Müller et al. (2005), (6) Martin et al. (1998) and (7) Anbar et al. (2007). Note that the depth is not to scale. (C) $^{147}Sm/^{144}Nd$ and $\varepsilon Nd_{(t)}$ data of the Turee Creek Group and Boolgeeda sediments. Bel Fm, Bellary Formation; MRB, Mt. Roe Basalt Formation; Hard Fm, Hardey Formation; Ky/Bo Fm, Kylena/Boongali Formation; Py/Tum Fm, Pyradie/Tumbiana Formation; Ma/Bu Fm, Maddina/Bunjinah Formation; Jeer Fm, Jeerinah formation; MMIF, Marra Mamba Iron Formation; NaM, Nammudi Member; MacL, MacLeod Member; MtN, Mt. Newman member; Witt Fm, Wittenoom Formation; Wan, West Angela Member; Para, Paraburdoo Member; BG, Bee Gorge Member; Mt Syl, Mt. Sylvia Formation; McRea, Mc Rae Shale; BRIF, Brockman Iron Formation; DGg, Dales Gorge Member; WSh, Whaleback Shale; Joff, Joffre Member; Yand, Yandicoogina Shale Member; WeWo, Weeli Wolli Formation; WRhy, Woongarra Rhyolites; Boo IF, Boolgeeda Iron Formation; MBM1- 2, Meteorite Bore Member; Kun, Kungarra Formation; K Fm, Koolbye Formation; Kaz, Kazput Formation; BRQ, Beasley River Quartzite; CSB, Cheela Springs Basalt; WD, Wooly Dolomite. (For interpretation of the references to colour in this figure legend, the reader is referred to the web version of this article.)

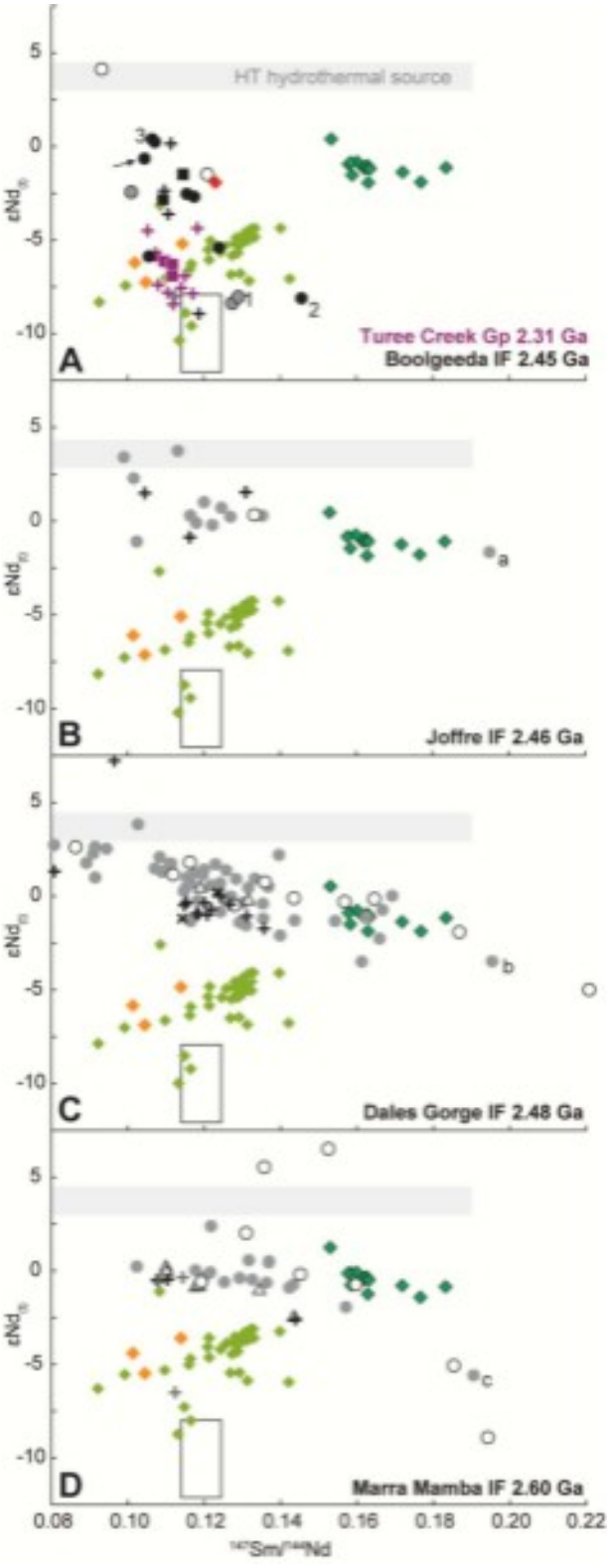

(caption on next column)

Fig. 3. $\varepsilon Nd_{(t)}$ vs $^{147}Sm/^{144}Nd$ cross-plots for the Turee Creek, Hamersley and Fortescue groups. Each diagram represents a snapshot of the different IFs and associated siliciclastic sediments of the Turee Creek and Hamersley basins at a given time. In each diagram, the Fortescue LIPs are shown as orange and green diamonds (see Fig. 1A for details) corrected for radioactive in-situ decay at each age of sediment deposition indicated in each diagram. The red diamond in diagram (A) corresponds to the 2.45 Ga old Woongarra Rhyolite. (A) Turee Creek Group and Boolgeeda Iron Formation sediments (this study). Symbols as in Fig. 2C. Black arrow indicates a sample of Boolgeeda IF analyzed by Alibert and McCulloch (1993) and numbers 1, 2 and 3 refer to the samples which REY patterns are shown in Fig. 4A. Joffre (B), Dales Gorge (C) and Marra Mamba (D) iron formations (Miller and O'Nions, 1985; Jacobsen and Pimentel-Klose, 1988; Alibert and McCulloch, 1993; Li et al., 2015) are shown as undifferentiated low-Al and high-Al IFs (grey dots), mudstone/siltstone (black crosses), chert (open dots) and carbonate (open triangles). In (C) black X represents two samples of McRae Shale and Whaleback Shale members (Alibert and McCulloch, 1993). In (D) open triangles correspond to carbonates of the Wittenoom and Jeerinah formations and dark grey crosses represent shales of the Jeerinah (near-chondritic $\varepsilon Nd_{(t)}$) and Hardey (negative $\varepsilon Nd_{(t)}$) formations. Letters a, b and c in Fig. 3B, C and D, respectively, refer to the samples which REY patterns are shown in Fig. 4B. In each diagram, the empty box represents the average composition of the modern upper continental crust (Chauvel et al., 2014) and data for the high temperature hydrothermal source are from Jacobsen and Pimentel-Klose (1988), Alibert and McCulloch (1993), Alexander et al. (2009), and Li et al. (2015). (For interpretation of the references to colour in this figure legend, the reader is referred to the web version of this article.)

and −4.0 and −8.9 and + 4.2, respectively (Fig. 3A). The positive $\varepsilon Nd_{(t)}$ value of about + 3 is typical of iron formations formed in seawater dominated by marine hydrothermal fluids (Alexander et al., 2009). Deviation towards negative values are generally interpreted to reflect the influence of a continental source material (e.g. Alexander et al., 2008). The recognition that both siliciclastic and chemical sediments define a single trend indicates that both physical and chemical weathering were active during deposition of the Boolgeeda IF and TCG sediments. The role of chemical weathering and its influence on riverine solute fluxes during deposition of the Boolgeeda IF is supported by the occurrence of IF samples showing typical REY seawater patterns and Al contents lower than 1 wt% but variable $\varepsilon Nd_{(t)}$ values between −2.4 and −8.1 (Fig. 3A and 4A). A secondary metamorphic/hydrothermal overprint is unlikely to explain this overlap between siliciclastic and chemical sediments as both high and low $\varepsilon Nd_{(t)}$ IFs preserve typical seawater-like REY patterns (Fig. 4A; see also discussion in Warchola et al., 2018). Additional evidence against a metamorphic/hydrothermal overprint comes from a variety of bulk and in situ isotopic studies (C, S, N, O, Fe) recently performed on the same drill core samples, which all point to the pristine character of the studied sediments (Philippot et al., 2018; Cheng et al., 2019; Killingsworth et al., 2019).

The relatively limited range of negative $\varepsilon Nd_{(t)}$ values of the TCG siliciclastic sediments compared to the Boolgeeda IF suggests that the TCG sediments derived from the erosion of a relatively homogeneous continental source, with no, or only limited, influence of a marine hydrothermal source. This is supported by trace element data, which show that the Boolgeeda IF samples with less than 1 wt% of Al_2O_3 display consistent LREE depletions, high Y/Ho ratios and positive La, Y, and Eu anomalies typical of seawater composition (Warchola et al., 2018). In contrast, the green mudstones and diamictite layer interbedded within the Boolgeeda IF and the grey mudstone/siltstones of the overlying Kungarra Formation display relatively flat normalized REE + Y patterns and lack anomalies characteristic of seawater. This has led Warchola et al. (2018) to interpret the Boolgeeda-Kungarra transition as a shallowing upward sequence associated with waning hydrothermal input and punctuated by intervals of detrital input. The nature of the weathered continental component can be further evaluated using the ternary mafic-felsic-weathering (MFW) diagram of Ohta and Arai (2007; Fig. 5). With the exception of the two chert samples (see below), the Boolgeeda IF plot close to the mafic-weathering tie-line, whereas the TCG samples

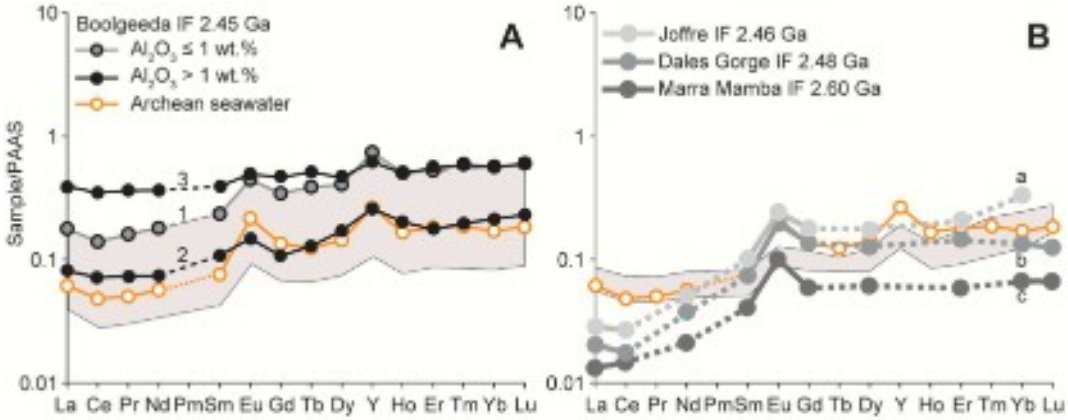

Fig. 4. REY_{PAAS} patterns for (A) Boolgeeda IF and (B) Joffre, Dales Gorge and Marra Mamba IFs. (A) REY data and grey field (Boolgeeda IF with $Al_2O_3 \leq 1$ wt%) are from Warchola et al. (2018) and numbers 1, 2 and 3 refer to the samples shown in Fig. 3A; (B) REY patterns from Alibert and McCulloch (1993) and grey field (analyses from Dales Gorge) from Pecoits et al. (2009). Small letters a, b and c refer to samples in Fig. 3B, C and D. White dots with orange contour defined as the Archean seawater, represent the average of the six best representative IFs samples ($Al_2O_3 \leq 1.5$ wt% and Ti < 150 μg/g) of the 2.95 Ga old Pongola Supergroup (Alexander et al., 2009). PAAS (Post Archean Australian Shale) values used for REY normalization are from Taylor and McLennan (2008). (For interpretation of the references to colour in this figure legend, the reader is referred to the web version of this article.)

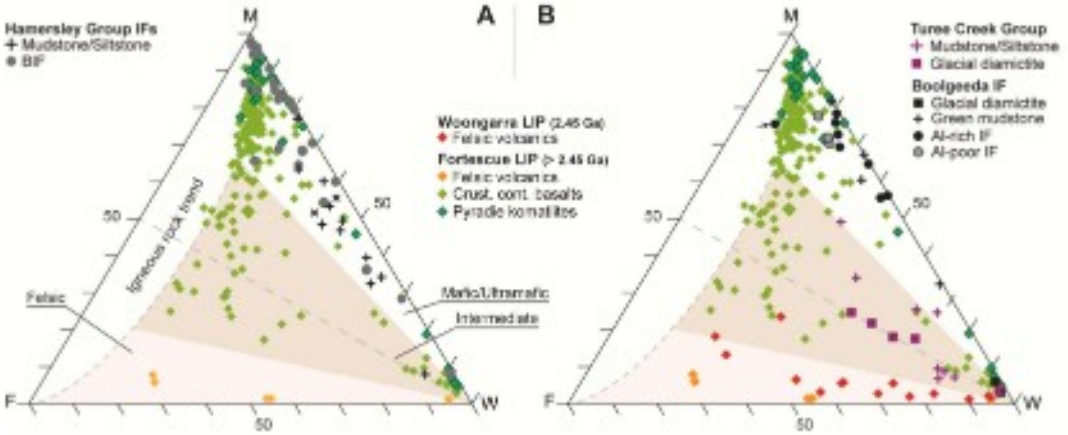

Fig. 5. Mafic-Felsic-Weathering (MFW) ternary diagram (Ohta and Arai, 2007) for the pre-GOE IF and associated siliciclastic sediments of the Hamersley Basin (A) and the *syn*-GOE Turee Creek and Boolgeeda sediments (B). MFW index was calculated using major elements of the TCG (Cheng et al., 2019), Boolgeeda IF (Warchola et al., 2018) and Hamersley IFs (Jacobsen and Pimentel-Klose, 1988; Alibert and McCulloch, 1993). Major elements for the Woongarra Rhyolites are from Trendall (1995), while those for the Fortescue LIPs are from Macfarlane et al. (1994a) and Mole et al. (2018, and references therein). In (A), the two black X represent two samples of McRae Shale and Whaleback Shale members (Alibert and McCulloch, 1993). In (B), the black arrow points to a sample of Boolgeeda IF analyzed by Alibert and McCulloch (1993). Crust. Cont. basalts: Crustally-Contaminated basalts.

show more intermediate to felsic compositions (Fig. 5B). This suggests that both mafic and felsic materials were delivered to the basin during deposition of the Boolgeeda and TCG sediments. As shown in Fig. 5B, different proportions of mafic/ultramafic and felsic subaerial volcanics of the underlying Fortescue and Woongarra Rhyolite (Macfarlane et al., 1994a; MacFarlane et al., 1994b; Trendall, 1995; Mole et al., 2018) can well explain the range of compositions recorded for the Boolgeeda and TCG sediments. The more felsic nature of the TCG sediments compared to the Boolgeeda glacial diamictites and mudstones indicates an increased influence of felsic sources with time, which can be accounted for by an increased contribution of an upper-crustal-like component to the TCG sediments (see Figs. 3 and 6). This interpretation is supported by the recent compilation of Warchola et al. (2018) who showed that the green mudstones were sourced from mafic lithologies such as Pilbara, Fortescue, and Weeli Wolli basalts, whereas the Kungarra diamictites and mudstone/siltstones appeared to be sourced from more felsic lithologies in the Hamersley Basin such as the Woongarra Rhyolite. The compositional link between the Boolgeeda IF and TCG samples and the underlying subaerial volcanics is also reflected in the older Joffre, Dales Gorge and Marra Mamba IFs and associated siliciclastic sediments (Alibert and McCulloch, 1993; Pecoits et al., 2009), which show the same range of mafic composition than the Boolgeeda IFs (Fig. 5B).

4.2. Comparison with Marra Mamba, Dales Gorge and Joffre IFs

Considering that the Hamersley IFs and TCG sediments were deposited in basins proximal to LIPs, and therefore could record the Nd signature of a dominantly mafic/felsic provenance, the influence of subaerial volcanics on the compositional budget of the Turee Creek and Hamersley sediments can be further constrained by comparing our data with previously published Nd-isotope data (Figs. 3 and 6; Miller and O'Nions, 1985; Jacobsen and Pimentel-Klose, 1988; Alibert and McCulloch, 1993; Li et al., 2015). The Nd-isotope compilation shown in Figs. 3 and 6 for iron formations, mudstone/siltstones and carbonates of the Hamersley Basin defines two main $\varepsilon Nd_{(t)}$ - $^{147}Sm/^{144}Nd$ negative trends of different slopes, which are best illustrated by the Boolgeeda IF-TCG (Fig. 3A) and the Dales Gorge IF (Fig. 3C), respectively. Joffre (Fig. 3B) and Marra Mamba (Fig. 3D) IFs show trends intermediate to

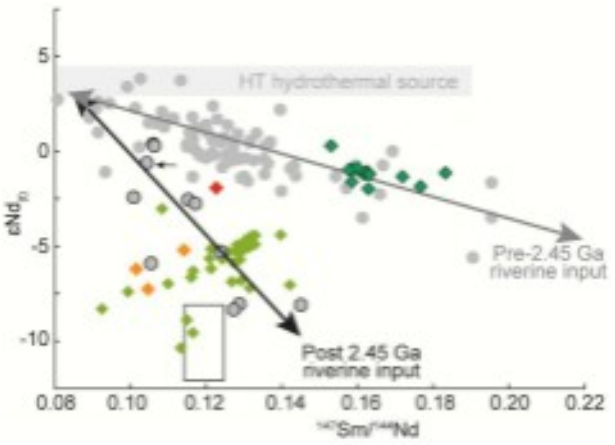

Fig. 6. $\varepsilon Nd_{(t)}$ vs $^{147}Sm/^{144}Nd$ cross-plot showing the shift of the seawater Nd isotopic composition in the Harmersley Basin at the onset of the GOE. Late Archean – Early Proterozoic IFs may reflect mixing of a hydrothermal source and a continental component (see text). The pre-2.45 Ga riverine input trend is defined by Joffre, Dales Gorge and Marra Mamba IFs (light grey dots) while the post 2.45 Ga riverine trend follows the Boolgeeda IFs (black contoured grey dots). Diamond symbols as in Fig. 1A and 3. The empty box represents the average composition of the modern upper continental crust (Chauvel et al., 2014).

Dales Gorge and Boolgeeda-TCG trends. In addition, one shale sample and two black shales and carbonate samples from the ~ 2.76 Ga old Hardey Formation and 2.68 Ga old Jeerinah Formation show Nd-isotope compositions overlapping the Boolgeeda-TCG trend (Fig. 3A and D; see below). In all sedimentary successions, several samples show extreme $\varepsilon Nd_{(t)}$ and $^{147}Sm/^{144}Nd$ values plotting outside these two main trends. These outliers are mainly represented by cherts and high-silica IFs (i.e. jasper). Cherts are distinguished from other sediments by low concentrations in almost all trace elements and their origin as primary or secondary chemical precipitates is still a matter of debate (e.g. Ledevin et al., 2014). A discussion of the geological significance of these specific samples is beyond the scope of this paper and will not be considered further here (but see Garçon et al., 2017; Warchola et al., 2018 for recent consideration on the origin of cherts). Nevertheless, these extreme values cannot be related to detrital contamination (e.g. Li et al., 2015) since IFs with the most negative $\varepsilon Nd_{(t)}$ and highest $^{147}Sm/^{144}Nd$ values contain less than 1 wt% of Al_2O_3 (Fig. 3B, C and D) and have seawater-like REY patterns compatible with those of the Archean Pietersburg IFs (Fig. 4B). This indicates that the Nd-isotopic composition of Hamersley seawater had some variability, likely due to differences in the Nd-isotopic composition of the sources.

A striking feature of the two trends defined by Boolgeeda and Dales Gorge IFs, is that they reflect the mixing between a marine hydrothermal source at $\varepsilon Nd_{(t)} \sim +3$ with two different continental components ($\varepsilon Nd_{(t)} \sim$ -9 and −4 and $^{147}Sm/^{144}Nd \sim 0.13$ and 0.18, respectively), which overlap the composition of the underlying Fortescue LIPs (Fig. 3A and C). Specifically, the trend defined by the Boolgeeda and TCG sediments overlap the 2.45 Ga old Woongarra Rhyolite (Figs. 1, 3A and 6; GSWA WAGeochem database) and some of the Fortescue subaerial volcanics mainly located in the northern part of the Hamersley Basin (Fig. 1A), which were shown to represent mafic to ultramafic magmas contaminated by the assimilation of highly-enriched 3.7 to 3.5 Ga continental crust of the underlying Pilbara Craton (Macfarlane et al., 1994a; Mac-Farlane et al., 1994b; Mole et al., 2018). As shown in Figs. 3 and 6, this crustally-contaminated mafic/ultramafic component overlaps in part the average composition of the upper continental crust (e.g., Chauvel et al., 2014). This indicates that a more diverse crustal component could also account for the Nd-isotope signature recorded in the Boolgeeda and TCG sediments. In contrast, Dales Gorge IF defines a trend intercepting the more radiogenic crustal component represented by the Pyradie komatiites deposited in the southern Hamersley Basin (Fig. 1A, 3C and 6; Mole et al., 2018). Joffre and Marra Mamba IFs define a trend very similar to Dales Gorge trend, but with several samples overlapping the Boolgeeda IFs (Fig. 3B and D). By examining Sm–Nd isotopes in the Hamersley IFs, Alibert and McCulloch (1993) reported a gradual change in the $\varepsilon Nd_{(t)}$ values from the lower Marra Mamba IF with $\varepsilon Nd_{(t)}$ values of − 0.6 to more positive εNd values of + 1 for the Dales Gorge and Joffre IFs. Nd mass balance calculations led these authors to suggest that mid-ocean hydrothermal fluids mixed with seawater could explain around 50% of the sourced Nd in Joffre IF. Similar conclusions were reached by Haugaard et al. (2016) using trace elements ratios. Differently from Alibert and McCulloch (1993), however, these authors argued for the prominent role of predominantly felsic volcanic fallouts in Joffre IF, which can be accounted for by the few IFs and siliciclastic samples plotting near the unique Woongarra Rhyolite sample analyzed for its Nd-isotope composition (Fig. 3A). In addition, the remobilization of sediments interbedded with subaerial volcanic units may represent a non-negligible weathering source component. This is supported by the unique Hardey shale sample analyzed by Alibert and McCulloch (1993), which shows a negative $\varepsilon Nd_{(t)}$ value of −6.4 at 2.6 Ga (Fig. 3D) and −8 at 2.45 Ga, in agreement with the Boolgeeda-TCG trend (Fig. 3A).

The interpretation that the TCG and Boolgeeda sediments could derive from the weathering of felsic and mafic/ultramafic sources that are only slightly older than their depositional age (between 2.45 and 2.2 Ga), agrees well with recent detrital zircon U-Pb ages and Hf isotope data obtained on the TCG and Boolgeeda sediments (Caquineau et al., 2020). As shown by these authors, the vast majority of the TCG and Boolgeeda detrital zircons analyzed yielded ages spanning those of the Hamersley and Fortescue groups between 2.45 and 2.78 Ga (Caquineau et al., 2018) and show supra-chondritic initial Hf isotopic compositions indicating that they crystallized in juvenile magmas. This U-Pb-Hf dataset can be well accounted for by the underlying Hamersley and Fortescue subaerial volcanic units, but not by the older crustal basements of the Pilbara Craton and Glenburgh Terrane, which formed the northern and southern borders of the Hamersley Basin during deposition of the Boolgeeda and TCG sediments. Alternatively, as discussed by Caquineau et al. (2020), the TCG - Boolgeeda zircons show some similarities with those of the northern Yilgarn Craton. Both display supra-chondritic $\varepsilon Hf_{(t)}$ values and a quite similar range of U-Pb ages. In addition, the occurrence of a Hadean zircon crystal in the Boolgeeda glacial diamictite, similar in age and Hf isotopic signature to the Jack Hills zircons (Whitehouse et al., 2017), makes the Yilgarn Craton a possible source for the Boolgeeda glacial horizon.

4.3. *Evolution of seawater Nd-isotope composition with time*

Because Nd isotopes are not sensitive to redox conditions, an important consequence for the interpretation of the shift in Nd-isotope compositions recorded in the pre-GOE and *syn*-GOE sediments (Fig. 6), is that it cannot be linked to a change in the weathering regime attending the rise of atmospheric oxygen at about 2.45 Ga, rather to a change in the nature and extend of the surface exposed to weathering. The trace element and Nd-isotope systematics discussed above for the Turee Creek and Hamersley sediments suggest that the composition of seawater in the Hamersley Basin was influenced by riverine solutes and clastic fluxes that derived from the weathering of different regions of the same subaerial volcanic province (Fig. 6). In this model, the shift in Nd-isotope compositions at about 2.45 Ga is linked to increased weathering of felsic and crustally-contaminated mafic/ultramafic subaerial volcanics due to a change in the geodynamic context of deposition and/or evolution of the hydrographic network and catchment areas. The timing of this shift coincides with the emplacement of the Woongarra Rhyolite and Weeli Wolly LIPs (Barley et al., 1997), which make them likely source material of the Turee Creek and Boolgeeda sediments. This is further supported by the recent Hf isotopic data obtained on detrital

zircons from the same samples than the one studied here, which showed that the Boolgeeda and the Turee Creek successions mainly derived from the erosion of the underlying Hamersley and Fortescue subaerial volcanics, with only minor contributions from the Pilbara Craton and the Glenburgh Terrane, which were located to the north and the south of the Hamersley Basin, respectively, at the time of deposition of the Turee Creek Group (Caquineau et al., 2020). Another explanation for the shift in Nd-isotope composition at about 2.45 Ga could be a significant change in the nature of fluid–rock interactions due to the increase role of weathering processes associated with the increase exposure of continental landmasses (Kump and Barley, 2007; Rey and Coltice, 2008; Bindeman et al., 2018). The emergence of vast landmasses would have led to expose larger surface and more diverse lithologies to weathering, resulting in a crustal component approximating the average composition of the upper continental crust (Figs. 3 and 6). The significant overlap between the zircon Hf isotope data of the Boolgeeda and TCG sediments and those of the Yilgarn Craton, together with the occurrence of a Hadean zircon crystal preserved in the Boolgeeda diamictite with similar age and Hf isotopic signature than the Jack Hills zircons, makes the Yilgarn Craton a possible source material for the Boolgeeda-TCG sediments (Caquineau et al., 2018, 2020). However, other cratons such as the Kaapvaal (South Africa) and Superior (North America) cratons show different zircons Hf data from the one recorded in the Turee Creek and Boolgeeda sediments, thus indicating that they did not contributed, at least significantly, to the Turee Creek and Boolgeeda sedimentation.

An alternative to the weathering models discussed above was recently proposed by Li et al. (2015). These authors argued that the continental source component defined by low-Al IFs with isotopically light $\delta^{56}Fe$ and negative $\varepsilon Nd_{(t)}$ values defining the "Dales Gorge trend" derived from the activity of Dissimilatory Iron Reducers (DIR) on the continental margins followed by transport through a microbial iron shuttle to the site of iron formations in deep basin environments. In this model, it is proposed that microbial dissolution of iron hydroxides in sediments is accompanied by significant REE fractionation, where the Fe (II)-rich pore waters possess significantly higher Sm/Nd ratios and Eu contents than the residual bulk siliciclastic sediments from which the Fe (II) was extracted from. This results in an increase in Sm/Nd ratios and Eu anomalies in pore fluids relative to bulk sediments at constant $\varepsilon Nd_{(t)}$ values. An important drawback with this model is that the source bulk sediments from which the Fe(II) is biologically extracted from was chosen with a constant $\varepsilon Nd_{(t)} = -3$, which incidentally match the most negative $\varepsilon Nd_{(t)}$ values of the Dales Gorge trend. However, as shown in Fig. 3, Dales Gorge and other Hamersley IFs are interbedded with siliciclastic sediments characterized by more positive, and most importantly variable $\varepsilon Nd_{(t)}$ values between + 2 and −2 (Alibert and McCulloch, 1993). It is therefore expected that Fe(II)-pore waters should carry a similar range of $\varepsilon Nd_{(t)}$ values and variable Sm/Nd ratios, which is not observed.

5. Conclusion

Our Nd-isotopic study indicates that weathering of the Late Archean subaerial flood basalts of the Fortescue Group dominated the continental detrital and chemical fluxes to the Hamersley Basin prior to about 2.45 Ga. $\varepsilon Nd_{(t)}$ values for shales that are coeval with IFs indicate that the Nd-isotopic composition of the crustal component changed abruptly at about 2.45 Ga, reflecting a change in the nature and extend of the continental surfaces exposed to weathering rather than a consequence of the rise of atmospheric oxygen. This change can be explained by the weathering of the immediately underlying felsic and crustally-contaminated mafic/ultramafic subaerial volcanics of the Fortescue and Hamersley groups. Alternatively, it may reflect a change in the hydrological cycle due to the increase contribution of riverine input to the basin attending emergence of surrounding landmasses. This increase exposure of continental surfaces could reflect a global increase of subaerial continental landmasses, which would have generated weathering products compositionally close to the modern upper crust. Additional data from other Paleoproterozoic cratons are needed, however, to evaluate if the change in Nd isotopic composition recorded in the Turee Creek and Boolgeeda sediments reflect a local process or a major change in the global hydrological cycle. Whatever the case, our data support the hypothesis that elevated rates of continental weathering contributed to the initiation of the first major rise of atmospheric oxygen and associated glaciations during the Archean-Proterozoic transition.

Declaration of Competing Interest

The authors declare that they have no known competing financial interests or personal relationships that could have appeared to influence the work reported in this paper.

Acknowledgements

This research was funded by Fundação Amparo à Pesquisa do Estado de São Paulo (FAPESP, grants 2015/16235-2, 2018/14617-3 and 2019/17732-0). We thank Olivier Bruguier for his assistance during Nd isotope analyses. We thank Shuan-Hong Zhang, Paul F. Hoffman and an anonymous reviewer for their constructive reviews.

Appendix A. Supplementary data

Supplementary data to this article can be found online at https://doi.org/10.1016/j.precamres.2021.106292.

References

Alexander, B.W., Bau, M., Andersson, P., 2009. Neodymium isotopes in Archean seawater and implications for the marine Nd cycle in Earth's early oceans. Earth Planet. Sci. Lett. 283 (1-4), 144–155.
Alexander, B.W., Bau, M., Andersson, P., Dulski, P., 2008. Continentally-derived solutes in shallow Archean seawater: Rare earth element and Nd isotope evidence in iron formation from the 2.9 Ga Pongola Supergroup, South Africa. Geochim. Cosmochim. Acta 72 (2), 378–394.
Alibert, C., McCulloch, M.T., 1993. Rare earth element and neodymium isotopic compositions of the banded iron-formations and associated shales from Hamersley, Western Australia. Geochim. Cosmochim. Acta 57 (1), 187–204.
Anbar, A.D., Duan, Y., Lyons, T.W., Arnold, G.L., Kendall, B., Creaser, R.A., Kaufman, A. J., Gordon, G.W., Scott, C., Garvin, J., Buick, R., 2007. A whiff of oxygen before the great oxidation event? Science 317 (5846), 1903–1906.
Arndt, N.T., Nelson, D.R., Compston, W., Trendall, A.F., Thorne, A.M., 1991. The age of the Fortescue Group, Hamersley Basin, Western Australia, from ion microprobe zircon U-Pb results. Aust. J. Earth Sci. 38 (3), 261–281.
Barley, M., Bekker, A., Krapez, B., 2005. Late Archean to Early Paleoproterozoic global tectonics, environmental change and the rise of atmospheric oxygen. Earth Planet. Sci. Lett. 238 (1-2), 156–171.
Barley, M.E., Pickard, A.L., Sylvester, P.J., 1997. Emplacement of a large igneous province as a possible cause of banded iron formation 2.45 billion years ago. Nature 385 (6611), 55–58.
Bindeman, I.N., Zakharov, D.O., Palandri, J., Greber, N.D., Dauphas, N., Retallack, G.J., Hofmann, A., Lackey, J.S., Bekker, A., 2018. Rapid emergence of subaerial landmasses and onset of a modern hydrologic cycle 2.5 billion years ago. Nature 557 (7706), 545–548.
Caquineau, T., Paquette, J.L., Gannoun, A., Philippot, P., 2020. Lu-Hf systematics of 4.0 – 2.3 Ga old zircons from the Turee Creek Group (Pilbara Craton, W. Australia): Implications on the rise of atmospheric oxygen and global glaciation during the Paleoproterozoic. Precambr. Res. 348, 105859.
Caquineau, T., Paquette, J.-L., Philippot, P., 2018. U-Pb detrital zircon geochronology of the Turee Creek Group, Hamersley Basin, Western Australia: Timing and correlation of the Paleoproterozoic glaciations. Precambr. Res. 307, 34–50.
Catling, D.C., Claire, M.W., 2005. How Earth's atmosphere evolved to an oxic state: A status report. Earth Planet. Sci. Lett. 237 (1-2), 1–20.
Chauvel, C., Garçon, M., Bureau, S., Besnault, A., Jahn, B.-M., Ding, Z., 2014. Constraints from loess on the Hf–Nd isotopic composition of the upper continental crust. Earth Planet. Sci. Lett. 388, 48–58.
Chauvel, C., Blichert-Toft, J., 2001. A hafnium isotope and trace element perspective on melting of the depleted mantle. Earth Planet. Sci. Lett. 190, 137–151.Cheney, E.S., 1996. Sequence stratigraphy and plate tectonic significance of the Transvaal succession of southern Africa and its equivalent in Western Australia. Precambr. Res. 190 (3-4), 137–151.
Cheng, C., Busigny, V., Ader, M., Thomazo, C., Chaduteau, C., Philippot, P., 2019. Nitrogen isotope evidence for stepwise oxygenation of the ocean during the Great Oxidation Event. Geochim. Cosmochim. Acta 261, 224–247.

Claire, M.W., Catling, D.C., Zahnle, K.J., 2006. Biogeochemical modelling of the rise in atmospheric oxygen. Geobiology 4 (4), 239–269.
Cox, G.M., Halverson, G.P., Stevenson, R.K., Vokaty, M., Poirier, A., Kunzmann, M., Li, Z.-X., Denyszyn, S.W., Strauss, J.V., Macdonald, F.A., 2016. Continental flood basalt weathering as a trigger for Neoproterozoic Snowball Earth. Earth Planet. Sci. Lett. 446, 89–99.
Flament, N., Coltice, N., Rey, P.F., 2008. A case for late-Archaean continental emergence from thermal evolution models and hypsometry. Earth Planet. Sci. Lett. 275 (3-4), 326–336.
Gaillard, F., Scaillet, B., Arndt, N.T., 2011. Atmospheric oxygenation caused by a change in volcanic degassing pressure. Nature 478 (7368), 229–232.
Garçon, M., Carlson, R.W., Shirey, S.B., Arndt, N.T., Horan, M.F., Mock, T.D., 2017. Erosion of Archean continents: The Sm-Nd and Lu-Hf isotopic record of Barberton sedimentary rocks. Geochim. Cosmochim. Acta 206, 216–235.
Haugaard, R., Pecoits, E., Lalonde, S., Rouxel, O., Konhauser, K., 2016. The Joffre banded iron formation, Hamersley Group, Western Australia: Assessing the palaeoenvironment through detailed petrology and chemostratigraphy. Precambr. Res. 273, 12–37.
Hoffman, P.F., 2013. The Great Oxidation and a Siderian snowball Earth: MIF-S based correlation of Paleoproterozoic glacial epochs. Chem. Geol. 362, 143–156.
Holland, H.D., 2002. Volcanic gases, black smokers, and the great oxidation event. Geochim. Cosmochim. Acta 66 (21), 3811–3826.
Jacobsen, S.B., Pimentel-Klose, M.R., 1988. A Nd isotopic study of the Hamersley and Michipicoten banded iron formations: the source of REE and Fe in Archean oceans. Earth Planet. Sci. Lett. 87 (1-2), 29–44.
Killingsworth, B.A., Sansjofre, P., Philippot, P., Cartigny, P., Thomazo, C., Lalonde, S.V., 2019. Constraining the rise of oxygen with oxygen isotopes. Nat. Commun. 10, 1–10.
Kump, L.R., Barley, M.E., 2007. Increased subaerial volcanism and the rise of atmospheric oxygen 2.5 billion years ago. Nature 448, 1033–1036.
Ledevin, M., Arndt, N., Simionovici, A., Jaillard, E., Ulrich, M., 2014. Silica precipitation triggered by clastic sedimentation in the Archean: New petrographic evidence from cherts of the Kromberg type section, South Africa. Precambr. Res. 255, 316–334.
Li, W., Beard, B.L., Johnson, C.M., Canfield, D.E., 2015. Biologically recycled continental iron is a major component in banded iron formations. Proc. Natl. Acad. Sci. 112, 8193–8198.
Macfarlane, A.W., Danielson, A., Holland, H.D., 1994. Geology and major and trace element chemistry of late Archean weathering profiles in the Fortescue Group, Western Australia: implications for atmospheric PO_2. Precambr. Res. 65 (1-4), 297–317.
MacFarlane, A.W., Danielson, A., Holland, H.D., Jacobsen, S.B., 1994. REE chemistry and Sm-Nd systematics of late Archean weathering profiles in the Fortescue Group, Western Australia. Geochim. Cosmochim. Acta 58 (7), 1777–1794.
Martin, D.M., Powell, C.M., George, A.D., 2000. Stratigraphic architecture and evolution of the early Paleoproterozoic McGrath Trough, Western Australia. Precambr. Res. 99 (1-2), 33–64.
Martin, D.M.B., 1999. Depositional setting and implications of Paleoproterozoic glaciomarine sedimentation in the Hamersley Province, Western Australia. Geol. Soc. Am. Bull. 111, 189–203.
Martin, D.M.B., Li, Z.X., Nemchin, A.A., Powell, C.M.A., 1998. . A pre-2.2 Ga age for giant hematite ores of the Hamersley province, Australia. Econ. Geol. 93, 1084–1090.
Mazumder, R., Van Kranendonk, M.J., Altermann, W., 2015. A marine to fluvial transition in the Paleoproterozoic Koolbye Formation, Turee Creek Group, Western Australia. Precambr. Res. 258, 161–170.
Miller, R.G., O'Nions, R.K., 1985. Source of Precambrian chemical and clastic sediments. Nature 314 (6009), 325–330.
Mole, D.R., Barnes, S.J., Yao, Z., White, A.J.R., Maas, R., Kirkland, C.L., 2018. The Archean Fortescue large igneous province: A result of komatiite contamination by a distinct Eo-Paleoarchean crust. Precambr. Res. 310, 365–390.
Müller, S.G., Krapez, B., Barley, M.E., Fletcher, I.R., 2005. Giant iron-ore deposits of the Hamersley province related to the breakup of Paleoproterozoic Australia: New insights from in situ SHRIMP dating of baddeleyite from mafic intrusions. Geology 33 (7), 577. https://doi.org/10.1130/G21482.110.1130/2005115.
Ohta, T., Arai, H., 2007. Statistical empirical index of chemical weathering in igneous rocks: A new tool for evaluating the degree of weathering. Chem. Geol. 240 (3-4), 280–297.
Pecoits, E., Gingras, M.K., Barley, M.E., Kappler, A., Posth, N.R., Konhauser, K.O., 2009. Petrography and geochemistry of the Dales Gorge banded iron formation: Paragenetic sequence, source and implications for palaeo-ocean chemistry. Precambr. Res. 172 (1-2), 163–187.
Philippot, P., Ávila, J.N., Killingsworth, B.A., Tessalina, S., Baton, F., Caquineau, T., Muller, E., Pecoits, E., Cartigny, P., Lalonde, S.V., Ireland, T.R., Thomazo, C., Van Kranendonk, M.J., Busigny, V., 2018. Globally asynchronous sulphur isotope signals require re-definition of the Great Oxidation Event. Nat. Commun. 9, 1–10.
Rasmussen, B., Fletcher, I.R., Sheppard, S., 2005. Isotopic dating of the migration of a low-grade metamorphic front during orogenesis. Geology 33 (10), 773. https://doi.org/10.1130/G21666.110.1130/2005153.
Rey, P.F., Coltice, N., 2008. Neoarchean lithospheric strengthening and the coupling of Earth's geochemical reservoirs. Geology 36, 635–638.
Taylor, S.R., McLennan, S., 2008. Planetary Crusts: Their composition, Origin and Evolution. Cambridge University Press, p. 378.
Teitler, Y., Le Hir, G., Fluteau, F., Philippot, P., Donnadieu, Y., 2014. Investigating the Paleoproterozoic glaciations with 3-D climate modeling. Earth Planet. Sci. Lett. 395, 71–80.
Trendall, A.F., 1979. A revision of the Mount Bruce Supergroup. W. Aust. Geol. Surv. Annu. Rep. 1978, 63–71.
Trendall, A.F., 1995. The Woogarra rhyolite - a giant lavalie felsic sheet in the Hamersley Basin of Western Australia. Western Aust. Geol. Surv. Report 42, 70 pp.
Trendall, A.F., Compston, W., Nelson, D.R., De Laeter, J.R., Bennett, V.C., 2004. SHRIMP zircon ages constraining the depositional chronology of the Hamersley Group, Western Australia. Aust. J. Earth Sci. 51 (5), 621–644.
Van Kranendonk, M.J., Mazumder, R., Yamaguchi, K.E., Yamada, K., Ikehara, M., 2015. Sedimentology of the Paleoproterozoic Kungarra Formation, Turee Creek Group, Western Australia: A conformable record of the transition from early to modern Earth. Precambr. Res. 256, 314–343.
Van Kranendonk, M.J., Mazumder, R., 2015. Two Paleoproterozoic glacio-eustatic cycles in the Turee Creek Group, Western Australia. Geol. Soc. Am. Bull. 127 (3-4), 596–607.
Warchola, T., Lalonde, S.V., Pecoits, E., von Gunten, K., Robbins, L.J., Alessi, D.S., Philippot, P., Konhauser, K.O., 2018. Petrology and geochemistry of the Boolgeeda Iron Formation, Hamersley Basin, Western Australia. Precambr. Res. 316, 155–173.
Whitehouse, M.J., Nemchin, A.A., Pidgeon, R.T., 2017. What can Hadean detrital zircon really tell us? A critical evaluation of their geochronology with implications for the interpretation of oxygen and hafnium isotopes. Gondwana Res. 51, 78–91.